Journal of Environment and Earth Science
ISSN 2224-3216 (Paper) ISSN 2225-0948 (Online)
Vol.3, No.14, 2013

Investigation of subsurface Geologic Features in Low latitude Crystalline Basement Complex: case study of Oke-Alapata Area, Ogbomoso, South-western Nigeria

Adabanija Moruffdeen[1*] Olasehinde Peter[1,2] Ologunaye Tosin[1] Ojetunde Abiodun[1]

1. Department of Earth Sciences, Ladoke Akintola University of Technology, Ogbomoso, Nigeria
2. Department of Geology, Federal University of Technology, Minna, Nigeria

* E-mail of the corresponding author: maadabanija@lautech.edu.ng

Abstract

Ground Magnetic survey has been carried out to investigate subsurface geology of Oke-Alapata area of Ogbomoso, Southwestern Nigeria. Magnetic measurements were recorded using proton precession magnetometer. The objectives of the research include determination of depth to magnetic source, investigation of subsurface reliefs and magnetic anomalies signatures associated with geological features such as joints, fractures and lithologic contacts as well as update the geology of the area.

The ground magnetic survey was preceded by geological mapping of the area. A total of ten profile lines were traversed in an east-west direction with an inter-profile spacing of 100m and station interval of 5m. The magnetic data obtained were processed and plotted on profiles to obtain the magnetic signatures of the subsurface. The data were subsequently interpreted qualitatively and quantitatively.

The geological mapping revealed the presence of migmatite-gneiss and quartzite at the northern and southeastern part respectively of the study area. The magnetic anomalies ranged from minimum negative peak value of -400nT to maximum peak value of 520nT. The detected geological features include joints and fractures as well as rock-rock contact between Migmatite-gneiss and quartzite. The depth to magnetic source ranged from 6.1m at the southeastern part to 10.8m at the northeastern part of the study area.

The strong correlation between the geological map of Oke Alapata, the identified geologic features and the magnetic anomalies interpretations has exemplified the use of magnetic anomalies signatures in characterizing geologic features in a low latitude crystalline basement complex studied.

Keywords: Ground Magnetic Survey, Subsurface Geology, Joints, Fractures, Rock-Rock contact, Ogbomoso, Nigeria

1. Introduction

In The magnetic method involves the measurement of the earth's magnetic field intensity. Typically the total magnetic field and/or vertical magnetic gradient is measured. Measurements of the horizontal or vertical component or horizontal gradient of the magnetic field may also be made. Anomalies in the earth's magnetic field are caused by induced or remanent magnetism. Induced magnetic anomalies are the result of secondary magnetization induced in a ferrous body by the earth's magnetic field. The shapes, dimensions, and amplitude of an induced magnetic anomaly is a function of the orientation, geometry, size, depth, and magnetic susceptibility of the body as well as the intensity and inclination of the earth's magnetic field in the survey area. It can be carried out on land (ground magnetic) or in air (aeromagnetic).

The magnetic method can be used to locate abandoned steel well casings, buried tanks, pipes and metallic debris (e.g. Frischknecht & Raab 1984; Frischknecht 1990); geothermal (Soengkono &Hochstein 1995); mapping of subsurface anomalies in an urban environment (Xia &Williams 2003, 2004; Xia et al. 2003, 2004); estimation of depth to basement and quantitative mapping of basement structures such as faults and horst blocks (Sunmonu et al. 2001; Prieto & Morton 2003; Sunmonu et al. 2004); heavy metal pollution (Schmidt et al. 2005); and archaeological sites investigation (Linford 1994; Schmidt 2001; Sternberg 2001; Sutherland & Schmidt 2003). The current study involves applications in the investigation of subsurface geology on the basis of anomalies in the Earth's magnetic field resulting from the magnetic properties of the underlying rock. The aim is to contribute to better understanding of the geology of Ogbomoso in south-western part of Nigeria which has been previously not well documented. Specifically, the objectives include: determination of depth to basement; determining the contact between rocks of different lithologic units; investigating subsurface relief and bedrock configuration; as well as correlation between geological structures and magnetic anomalies. The study area is located at Oke-

Alapata area of Ogbomoso, South-Western Nigeria (Figure 1). It has an aerial extent of approximately 6.5 square kilometers and is bounded by the geographic coordinates; latitude 08^0 $6^/$ N to 08^0 $7^/$ N and longitude 004^0 $13^/$ E to 004^0 $14^/$ E respectively (Figure 2). The topography is flat with River Ora as the major river with three tributaries (Figure 2).

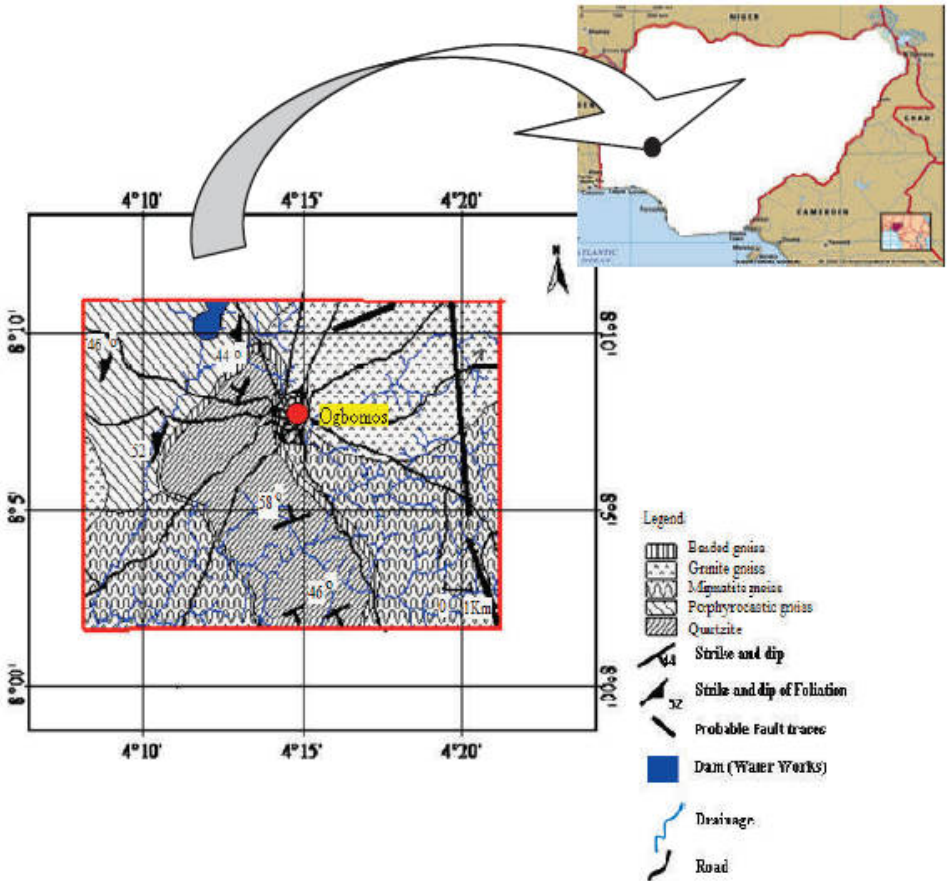

Figure 1. Geological map of Ogbomoso, inset : map of Nigeria (modified after Afolabi *et al.*, 2013)

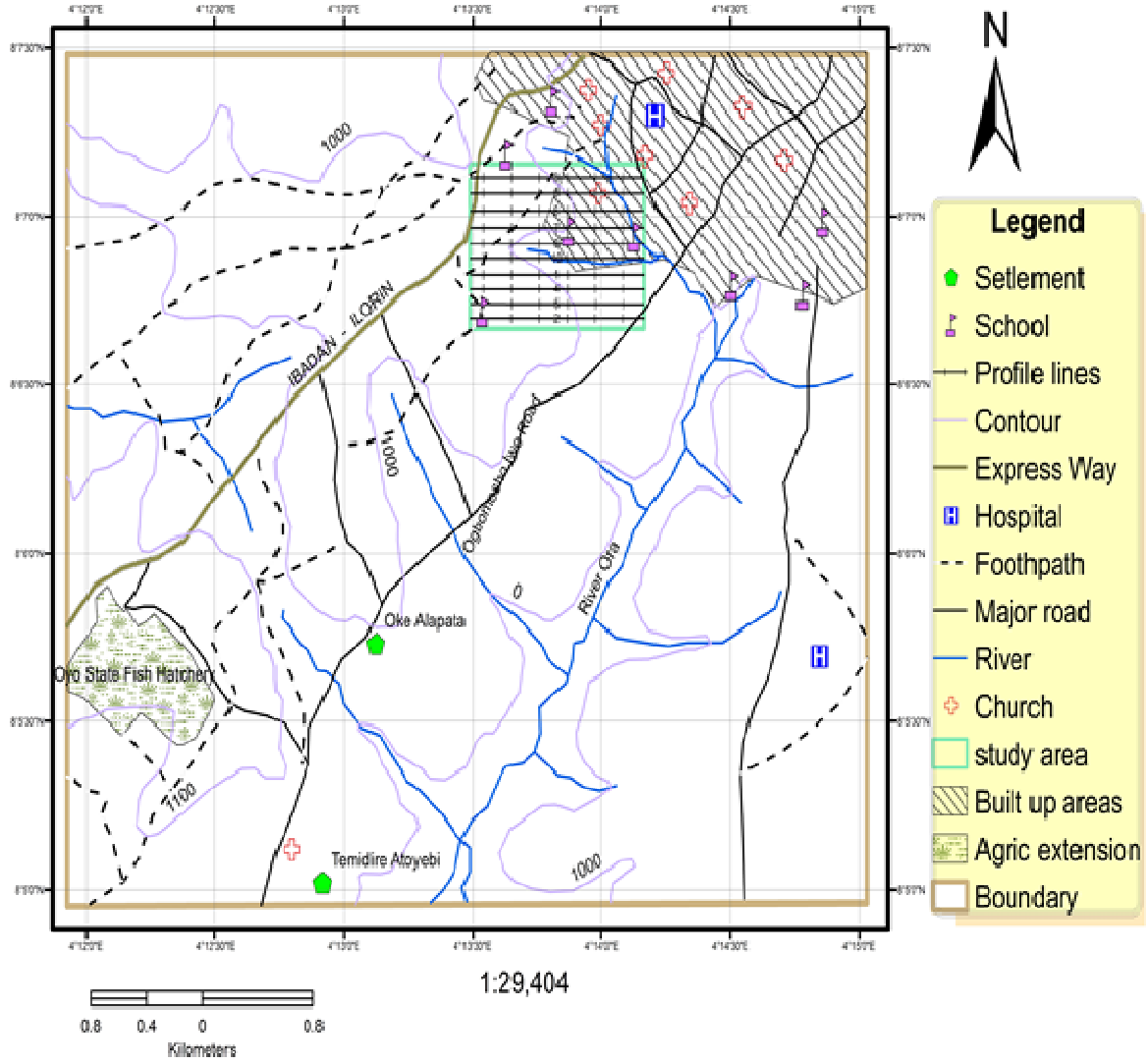

Figure 2. Location Map of the study area showing the drainage pattern and Profile lines

2. Theory

The Earth's magnetic field is believed to be generated by shearing and twisting fluid motions created by magneto-hydrodynamic process within the liquid, electrically conducting outer core of the earth. The resulting dynamo generates induction currents which subsequently generate the earth's magnetic field (Telford et al.1976; Keary et al. 2002). The field is manifested as a smoothly varying dipolar field with south and north magnetic poles roughly aligned with the earth's geographic north and south poles, respectively.

The earth's magnetic field is a vector field, specified at a given location by the magnitude of the magnetic force (total field intensity) and its direction. Declination (the angle between geographic north and magnetic north) and inclination (the angle of dip) describe the direction of the field at a given point (Figure 3).

The magnetic field of the earth is not constant in time. Movement of ionized particles in the atmosphere creates irregular electrical currents that induce secondary magnetic fields. These daily changes are called the diurnal variation. The amplitude of the diurnal variation ranges from about 20 nT to 50 nT on a daily cycle. Magnetic storms due to sunspot activity often cause extreme disturbances in the magnetic field over periods of days to weeks. Further, secular (long-term) variation of the field occurs over periods of years to thousands of years. For reasons not entirely clear, the magnetic field has changed polarity, as well, many times throughout earth's history.

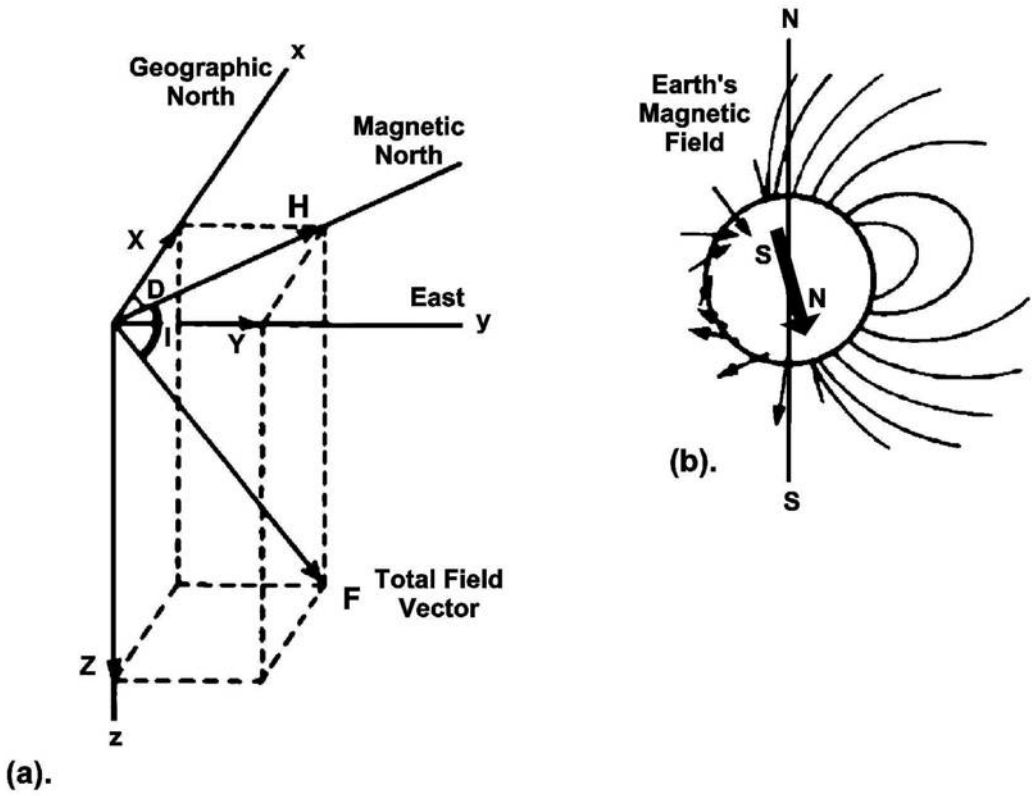

Figure 3. Schematic diagram showing (a) the components of the earth's magnetic field vector at the surface in northern, midlatitudes: D, declination; I, inclination; H, horizontal component; Z, vertical component; F, total field vector. (b). the Earth's dipolar field (modified after Hinze 1990).

The magnetic method involves measuring some component of the magnetic field near the surface of the earth. Small spatial variations in the shape of the field near the earth's surface reflect conditions in the subsurface. These local variations, with respect to a smoothly varying regional component, are referred to as magnetic anomalies. Delineation and interpretation of the source of magnetic anomalies is the primary objective of most magnetic surveys.

A magnetic anomaly is generated only when there are lateral variations in magnetic susceptibility k, i.e. it is a susceptibility contrast that causes an anomaly and it is the proportionality factor by which the induced intensity of magnetization depends on the strength of the magnetizing force H of the inducing geomagnetic field. This proportionality between the magnetization M and the magnetizing field H is expressed by:

$$M = kH \quad (1)$$

The measured parameter of magnetic surveys is the total magnetic field, which is the magnetic induction B (measured in nT) including the effect of magnetization M. It can be written as:

$$B = \mu_o(H + M) \quad (2)$$

However, by inserting equation (1) into equation (2)

$$B = \mu_o(1 + k)H = \mu\mu_o H \quad (3)$$

Where $\mu_o = 4\pi \times 10^{-7}$ H/m the permeability of free space.

3. Geological Setting

Oke-Alapata is located in Ogbomoso, southwestern Nigeria Precambrian Basement Complex. The rock units comprise ancient gneiss-migmatite series e.g gneiss; meta-sedimentary series namely quartzite and quartz-schists; and older granites (Jones & Hockey 1964; Rahaman 1989). The gneisses are the most dorminant rock type and occur mainly as granite gneiss and banded gneiss with medium to coarse-grained textures and no definite

foliation pattern. They contain biotite, hornblende, quartz, plagioclase, microcline and rarely pyroxene. The quartzite occur as long elongated ridge from the south and terminate with porphyro-blastic gneiss at the northeast (Figure 1) and mostly massive schistose quartzites with micaceous minerals alternating with quartzo-feldspathic rocks which are common in the southern part of the town. The older granites consist of medium to coarse-grained porphyritic granites, granodiorite, biotite granites and affiliated minor rocks such as pegmatites. Pegmatites are common as intrusive rocks occurring as joints and vein fillings. They are coarse grained and weathered easily into clay and sand-sized particles, which serve as water bearing horizon of the regolith.

4. Methodology

4.1 Data Acquisition

The ground magnetic data (magnetic intensity values) were acquired during the months of September to November 2009 using manual push-button proton precession magnetometer. This was preceded by geological mapping in January/February 2009. A total of ten profiles were traversed along east-west direction (Figure 2) with station interval of 5m for each profile. The length of the profiles varied from about 450m to 1200m depending on space availability. The inter-profile spacing was 100m along North-South direction resulting to aerial extent of approximately 6.5km^2.

Base stations were established at the middle of each profile and divided into east and west directions. The readings at base stations were taken at an interval of 20 minutes to 30 minutes for each profile. GPS coordinates were also taken at appropriate places.

4.2 Data Processing

The magnetic intensity values obtained were subjected to Secular variation Diurnal variation, and magnetic storm corrections. These were achieved by reading the magnetometer value at a fixed base station periodically throughout the day. The differences observed in base reading were then distributed among the readings at station occupied during the day according to the time of observation. The corrected data were used to plot the variation of magnetic susceptibility along each profile.

4.3 Data Interpretation

The corrected magnetic values observed were subjected to both qualitative and quantitative interpretation. Qualitative interpretation was made by visualizing the magnetic contour map constructed and involved examination of the general trend of the contours to infer the likely geologic features. Each profile was also qualitatively interpreted to identify associated geologic and structural features and magnetic anomalies signatures. This was accomplished by dividing the magnetic contour values into three classes (Olasehinde 1990) according to magnetic susceptibilities of the rock types in the project area. These are;

- Areas of high magnetic susceptibility values (magnetic high); 100nT and above.
- Areas of intermediate magnetic susceptibility values; -100nT to 100nT.
- Areas of low magnetic susceptibility values (magnetic low); below 100nT.

For quantitative interpretations, Pal's (1984) method was used to calculate the depth to magnetic source and involved the following step-wise procedure:

4.3.1Construction of Derived Profile

Derived profile is the new profile produced from the observed profile to serve as a check and was used to obtain the estimate of depth to magnetic source. It involved the construction of horizontal and vertical lines. The horizontal lines were constructed by averaging the corresponding magnetic intensity values of the crests and troughs of the observed profiles. The horizontal line divides the crest and trough and was used to get the mid-point value that was also used in the observed profile (Figure 4).

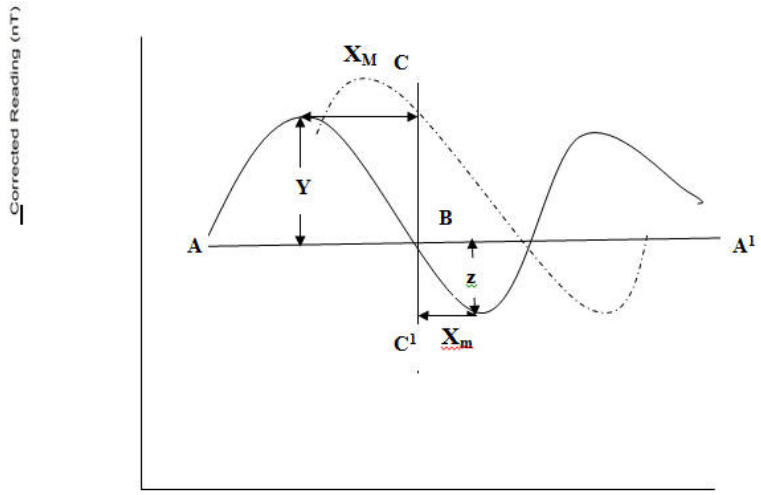

Figure 4. Features of generalized graph profile, AA^1 constructed horizontal scale, B epicentral position, CC^1 constructed vertical Scale, Y crest region, Z trough region, dash line derived profile, X_M measured maximum displacement, X_m measured minimum displacement (Poorna, 1984)

A vertical line which is perpendicular to the horizontal line was also drawn passing through the mid-point. This point of division is called the epicentral position. Values within the crest regions were assigned positive while those within the trough regions were assigned negative values.

On the horizontal line, a scale which increases numerically was constructed from the first point of contact to the last point of contact of the horizontal line with the sinusoidal curve. The first point of contact was assigned zero and it increases numerically to the last point of contact. The constructed values in this horizontal scale were traced to the point of intersection with the plotted graph and their corresponding magnetic anomalies were recorded.

The recorded magnetic anomalies were subtracted in turn in a cumulative manner to give the differential magnetic anomaly $X\text{-}X_0$. The differential anomalies were divided by station spacing interval to obtain the values of the vertical scale. The values of the horizontal scale were plotted against the corresponding values on the vertical scale to eventually obtain the derived profile corresponding to the observed profile (Figure 4).

4.3.2 Estimation of Depth to Basement

It should be noted from Figure 4 that X_m values are negative while X_M values are positive. Hence, the epicentral position (X_o) is the point at which X = 0. The derivative profiles further help in determining the precise value of X_m and X_M after the epicentral position has been located. These minimum and maximum values were then used in determining the parameter U. Where U is the square root of multiples of minimum and maximum values as shown among the following parameters;

- m = minimum value of anomaly of chosen curve
- M = maximum value of anomaly of chosen curve
- $X = X_o = m + M / 2$ = epicentral position
- Xm = Measurement of minimum displacement
- X_M = Measurement of maximum displacement

The above parameters were manipulated and resolved via various mathematical equations to obtain the depth to magnetic source.

$$U = \sqrt{-X_m X_M} \quad (4)$$

From equation 4 (the negative sign only implies minimum displacement as on Figure 4), the depth to burial can

then be calculated using the equation below;

$$\theta_F = \pm \tan^{-1} B \sqrt{\frac{\bar{U}}{X_m + X_M}} \quad (5)$$

Where θ_t is a function of depth to basement parameters; B is a constant dependent on the method of estimation.

For Poorna's method, B=1.1457

The depth to basement h was eventually calculated using;

$$h = \pm \tfrac{1}{2} (X_m + X_M) \tan \theta_t \quad (6)$$

A sample calculation is as in appendix I.

Due to rigorous mathematical manipulations and substitutions as well as the size of the profiles involved, a computer implementation procedure employing JAVA language was developed and is as in appendix II. The data capture platform of the program is shown in Figure 5.

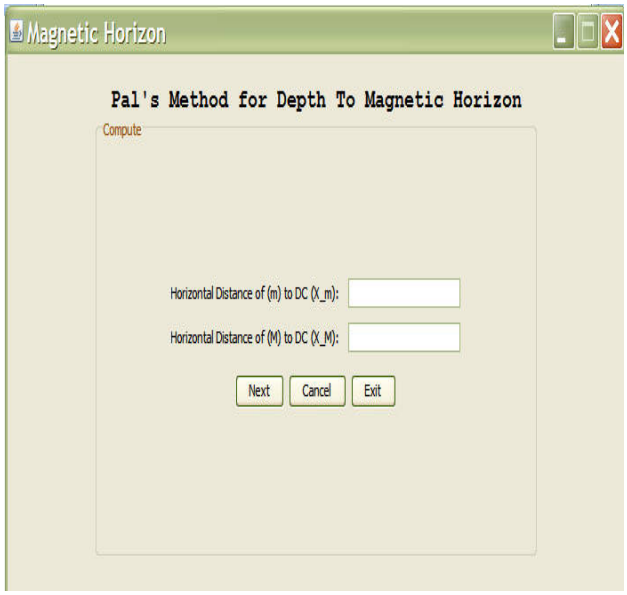

Figure 5. Data capture platform for the determination of depth to magnetic horizon

5. Results and Discussion

5.1 Geological Mapping

5.1.1 Lithology

The geologic map of Oke-Alapata obtained from geological mapping is as shown in Figure 6. It indicated that the area is predominantly made up of migmatite-gneiss and quartzite with their contact trending SSW-NNE.

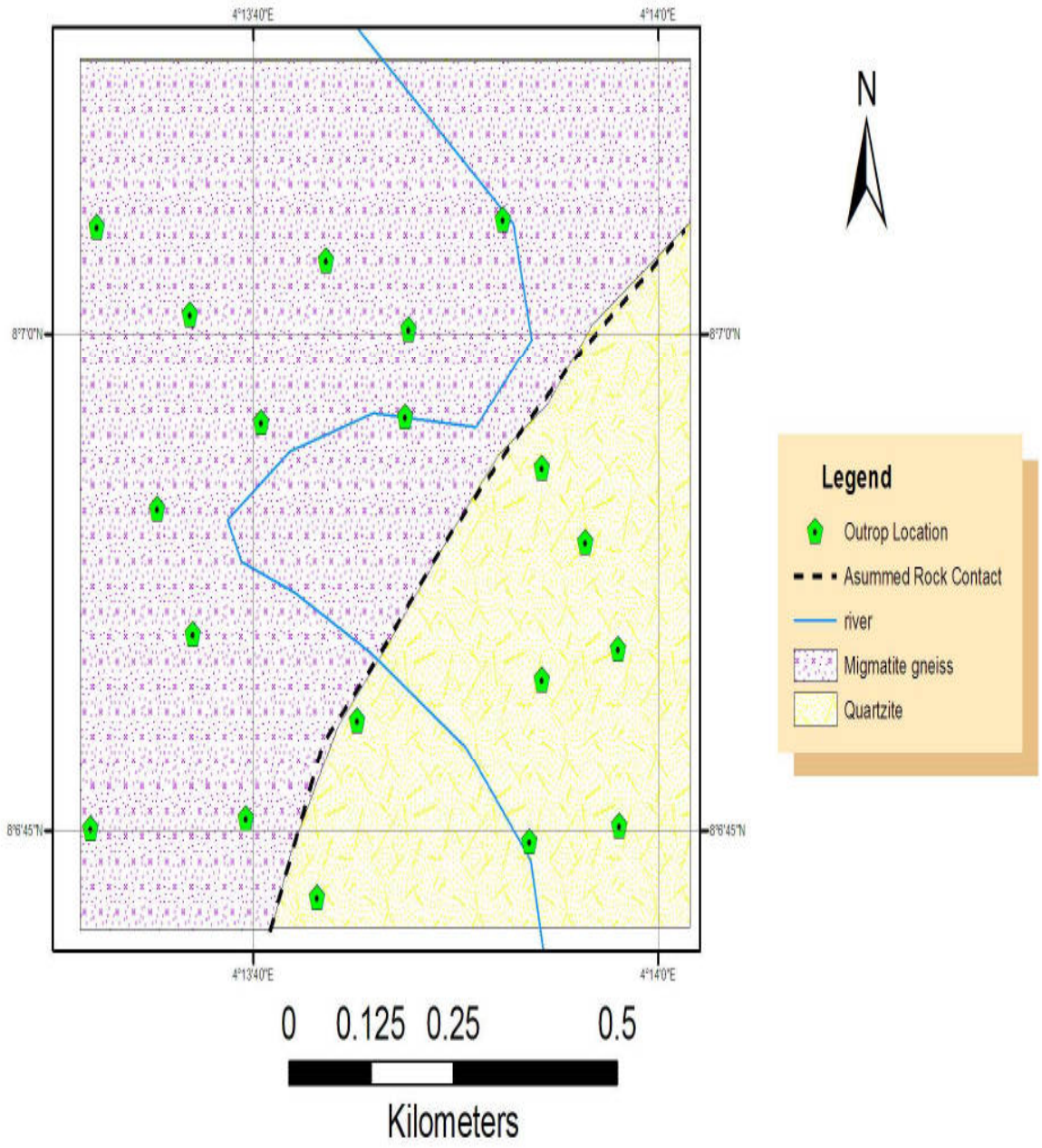

Figure 6. Geological Map of the Study Area Obtained from Surface Field Mapping

The quartzite was light brown in colour and medium to coarse-grained in texture (Figure 7a), though fresh samples revealed a whitish colour which was also slightly pink due to the presence of potassium feldspar in the rock. Some areas also showed a dark brown coloration which could be due to weathering effects. The rock exhibited conchoidal fracture typical of the quartz minerals, with a number of joints and no visible foliation. The quartz schist is most likely formed by low-grade regional metamorphism.

Figure 7. Lithology and some geologic structures at Oke Alapata, South-western Nigeria (a) Quartzite; (b) Migmatite gneiss; (c) Fracture; (d) Joint

The migmatite-gneiss consists of quartz and feldspar with some noticeable mica (Figure 7b). Schistocity and banding are poor, irregular and discontinuous. It occurs as the country rock with regional strike NNW-SSE.

5.1.2 Structural Features

Few of the exposures in the study area were jointed especially quartzite which exhibits conchoidal fractures typical of the quartz minerals, with a number of joints and no visible foliation. The migmatite-gneiss also exhibit joints. There were also intrusive igneous bodies which intrude concordantly into Migmatite-gneiss forming a sill.

Quartz vein occurs in some of the migmatite-gneiss outcrops, emplaced along joints and veining through the rocks in different directions. Its dimension varies from 5mm to 3cm and the grain size is generally medium – coarse. These structural features are shown in Figure 7c and Figure 7d.

5.2 Ground Magnetic Survey

5.2.1 Qualitative Interpretation

The magnetic susceptibility profile plots of the area are as shown in Figures 8a-j.

Profile One (East - West)

The eastern part of profile one (Figure 8a) consists of areas of intermediate magnetic susceptibility values

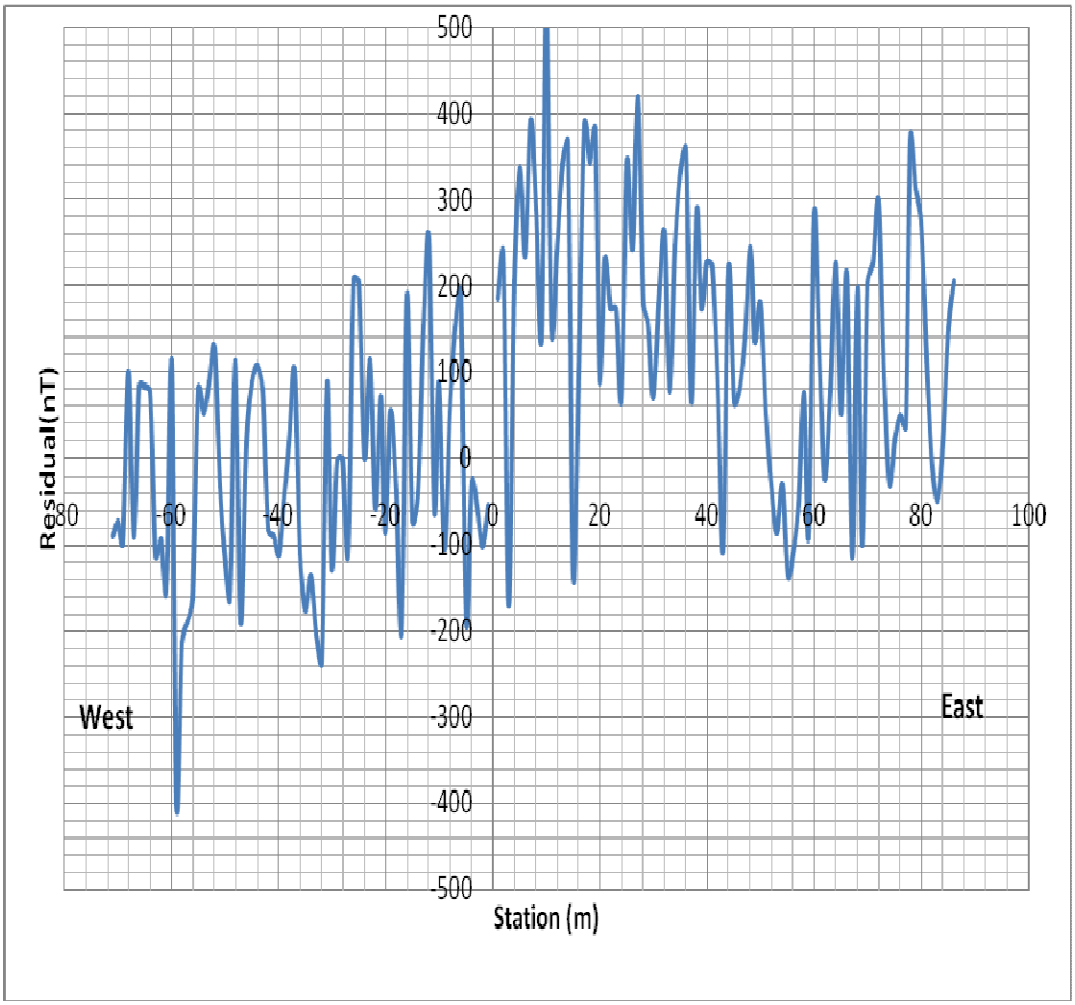

Figure 8a. Magnetic Susceptibility Profiles along Profile 1.

and magnetic highs. These areas with high magnetic gradient usually correspond with areas having closely packed contour on a contour map and may be associated with rocks of high magnetic content and situated close to the surface. There is also a slight variation in the anomaly value from magnetic high to magnetic low as we move away from the base station. The high negative magnetic anomaly values may indicate faults or fractures while the transition may be due to rock-rock contact around the base station probably between the quartzite body and the migmatite-gneiss of the study area.

At the western part of the profile, the subsurface mostly consist of rocks of intermediate magnetic susceptibility values. It also has some magnetic lows corresponding to magnetic source at great depth.

Profile Two (East – West)

The profile is about 625m long (Figure 8b). The magnetic susceptibility ranged from intermediate to low. However there is an area of high magnetic gradient at the eastern end between stations 55 and 65 which may be due to an intrusion. The intermediate magnetic values correspond to the regional susceptibility of the area. The magnetic lows are probably due to deeply concealed magnetic source.

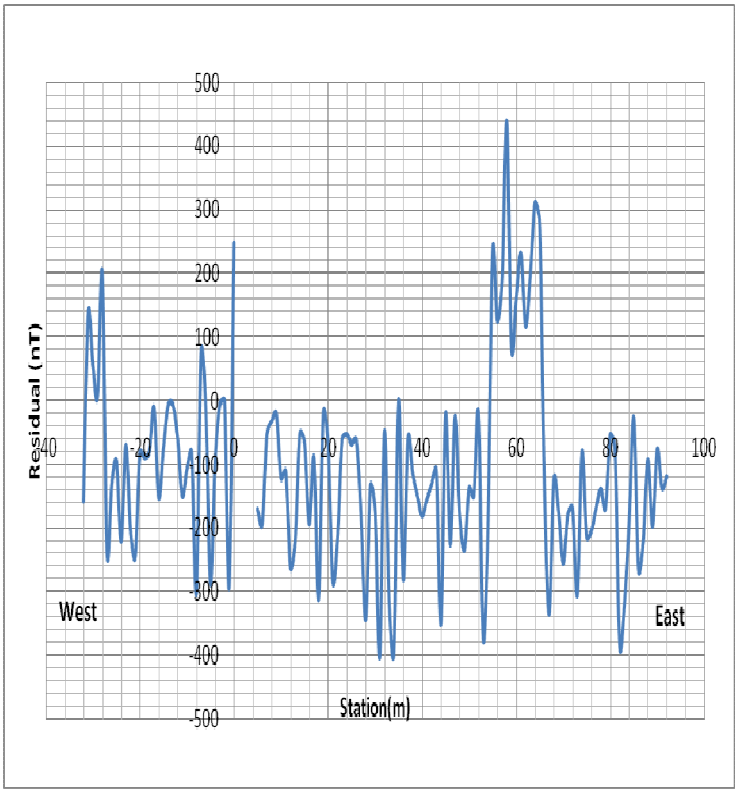

Figure 8b. Magnetic Susceptibility Profiles along Profile 2

Profile Three (East - West)

The profile is about 550m long. The subsurface mostly exhibit magnetic susceptibility values of the regional magnetism of the study area (susceptibility values between -100nT and 100nT) as shown in Figure 8c. There are also areas of magnetic lows indicating that the magnetic source is relatively at great depth.

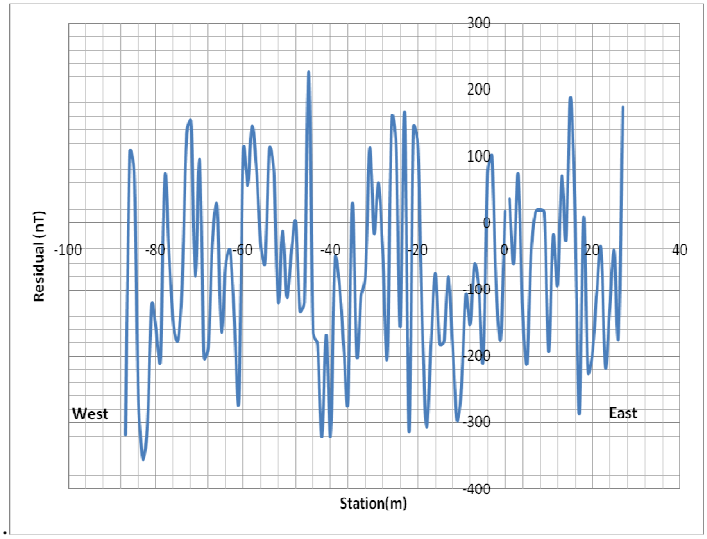

Figure 8c. Magnetic Susceptibility Profiles along Profile 3

Profile Four (East - West)

Profile four is about 750m long. The Eastern part of this profile dominantly has high magnetic susceptibility values indicating the source rock is at shallow depth. The high magnetic susceptibility values may also be due to intrusive igneous bodies concordantly intruding into the country rock. This is as indicated in Figure 8d

The western part of the profile comprises areas of intermediate magnetic susceptibility values. There are also few points of magnetic highs but these are not as extensive as those of the eastern part of this profile. This may

indicate rock-rock contact.

.

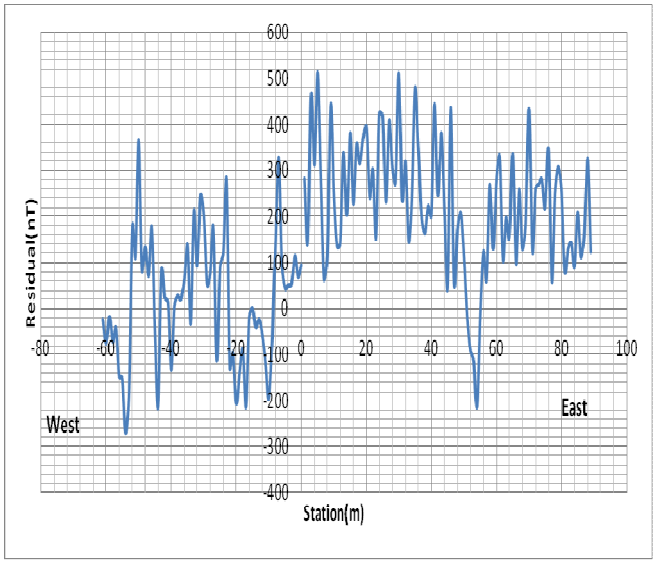

Figure 8d. Magnetic Susceptibility Profiles along Profile 4

Profile Five (East – West)

Profile five comprises areas of high magnetic values (Figure 8e). The profile is about 400m long. The highest magnetic value is about 380nT while the lowest magnetic value is about -250nT. These areas with high magnetic gradient usually correspond with areas having closely packed contour on a contour map and may be associated with rocks of high magnetic content and situated close to the surface.

The western part of the profile indicates intermediate to low magnetic values indicating little quantities of ferromagnesian materials/minerals. The magnetic lows are probably due to deeply concealed magnetic source.

There is most likely to be a rock-rock contact around the base station of the profile probably between the quartzite body and the migmatite-gneiss of the study area.

Profile Six (East - West)

The profile is about 1050m long. On the eastern part, from the base station to station 40 (about 200m) indicate dominantly magnetic highs (Figure 8f). This may be associated with rocks of high magnetic content and situated close to the surface. From about 200m to the end of the profile, there is a gradual decrease in the magnetic content. The rock type in this area is mostly of high magnetic anomaly values. The western part of the profile contains rocks of intermediate to low magnetic susceptibility values.

Profile Seven (East - West)

Profile seven is about 850m long. The eastern part of the profile is mostly made up of rocks exhibiting the regional magnetic susceptibility trend of the study area (intermediate magnetic susceptibility values). There

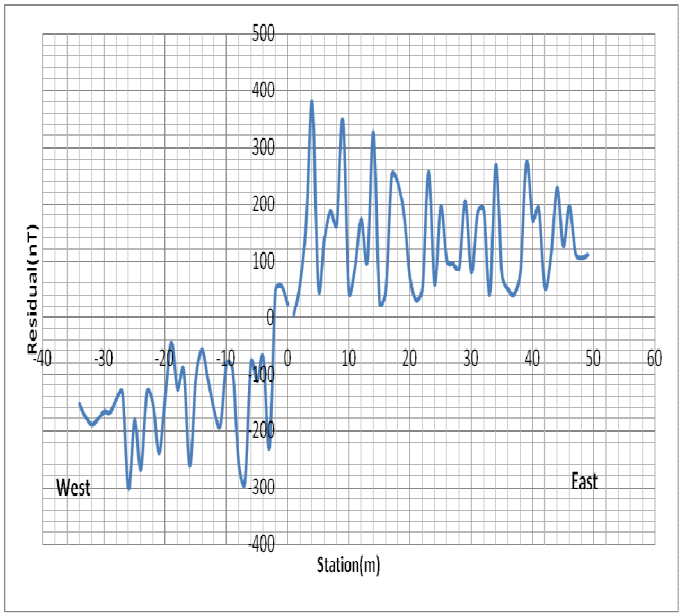

Figure 8e. Magnetic Susceptibility Profiles along Profile 5

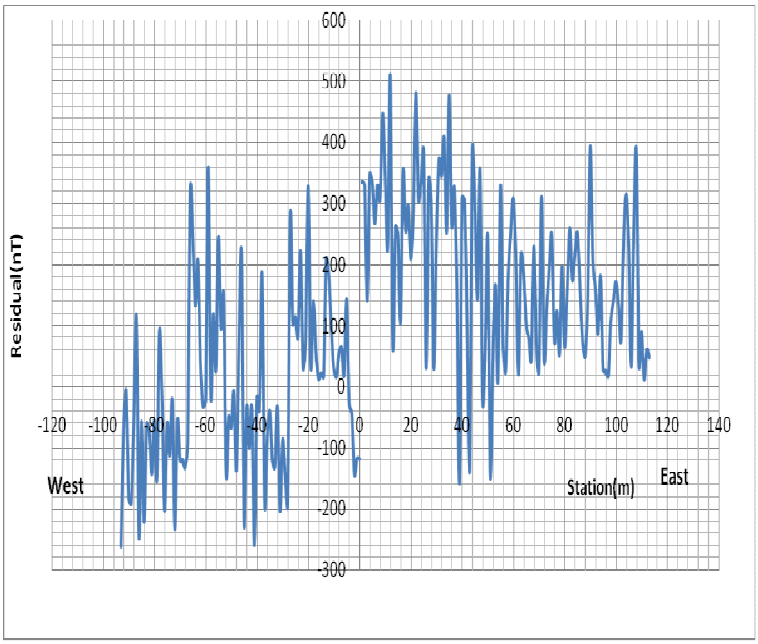

Figure 8f. Magnetic Susceptibility Profiles along Profile 6

are also areas of magnetic highs and magnetic lows (Figure 8g). The magnetic highs may be associated with rocks of high magnetic content which are situated close to the surface while the magnetic lows are probably due to deeply concealed magnetic source.

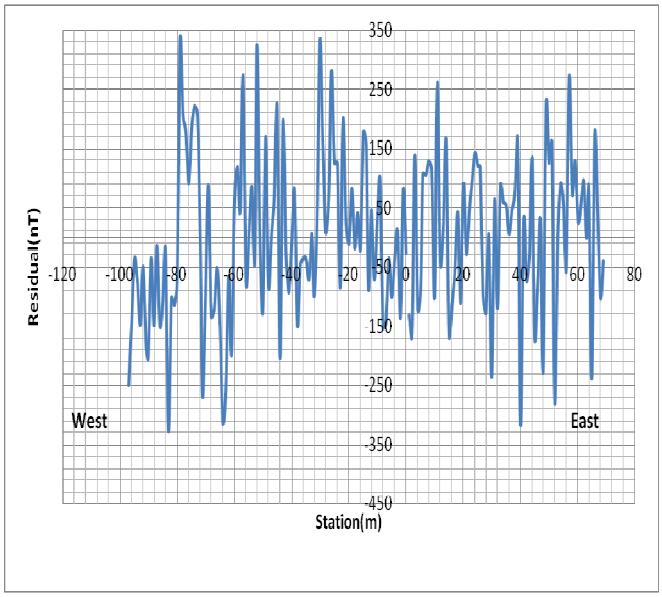

Figure 8g. Magnetic Susceptibility Profiles along Profile 7

Profile Eight (East - West)

Profile eight covers an area of about 800m. The eastern part of profile eight contains mostly of low magnetic anomaly values probably due to deeply concealed magnetic source. The western part of the profile mostly contains rocks of intermediate magnetic susceptibility values (regional magnetic susceptibility of the study area) as illustrated in Figure 8h. The rock types are of intermediate to high magnetic anomaly values. The high anomaly values are as a result of shallow concealed magnetic source.

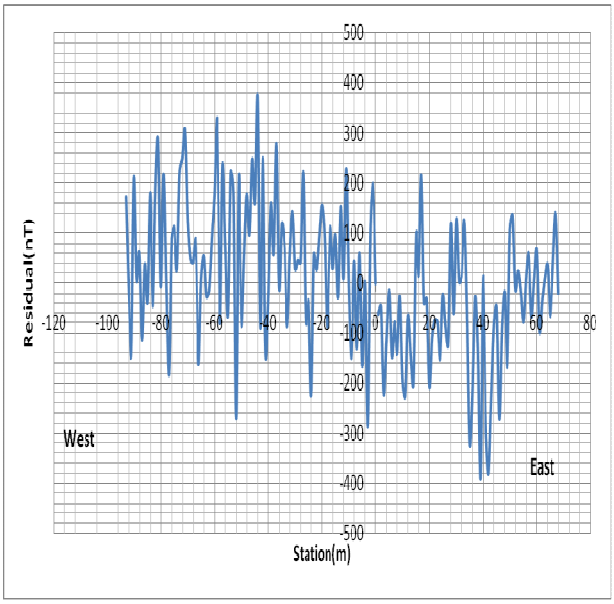

Figure 8h. Magnetic Susceptibility Profiles along Profile 8

Profile Nine (East - West)

Profile nine is mostly made up of rocks exhibiting the regional magnetic susceptibility trend of the project area. The profile is about 800m long (Figure 8i). There are also areas of magnetic highs and magnetic lows. The magnetic highs may be associated with rocks of high magnetic content which are situated close to the surface while the magnetic lows are probably due to deeply concealed magnetic source.

In the western part of the profile, there is a gradual increase in the magnetic materials as we go towards the end of the profile. This is probably due to shallow concealed magnetic source.

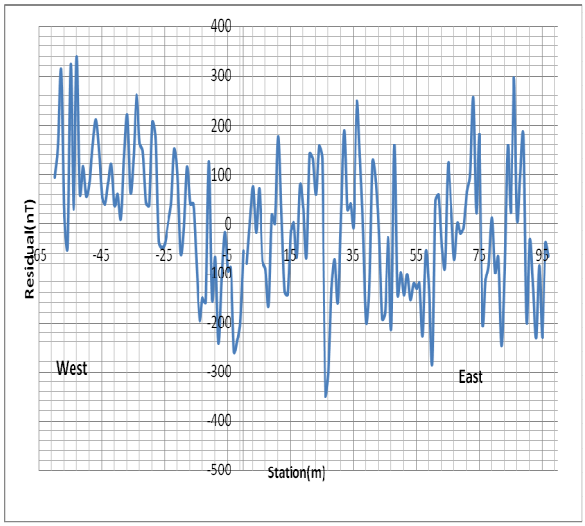

Figure 8i. Magnetic Susceptibility Profiles along Profile 9

Profile Ten (East - West)

Profile ten covers an area of about 750m. The profile mainly contains rocks of low magnetic susceptibility values (Figure 8j). The low magnetic anomaly values may be as a result of deeply concealed magnetic source.

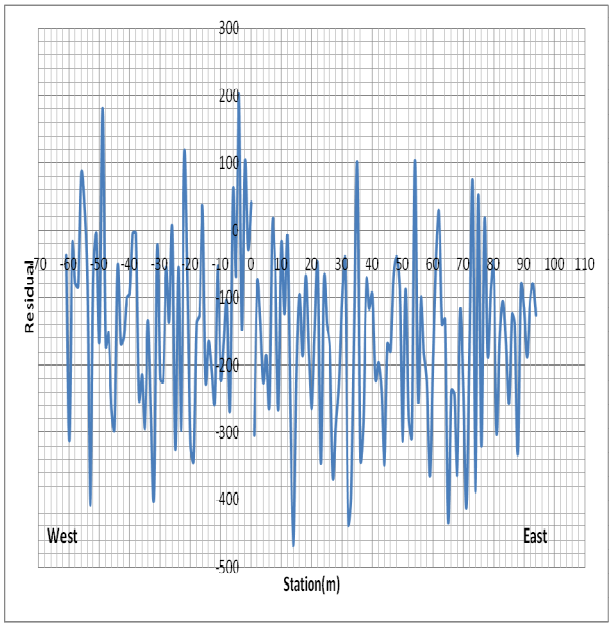

Figure 8j. Magnetic Susceptibility Profiles along Profile 10

The geological map obtained based on the above interpretation and superimposition of the magnetic signature on the base map of the study area is as shown in Figure 9. The map indicates the migmatite-gneiss dominated the northern and the southwestern parts while the remaining part was dominated by quartzite.

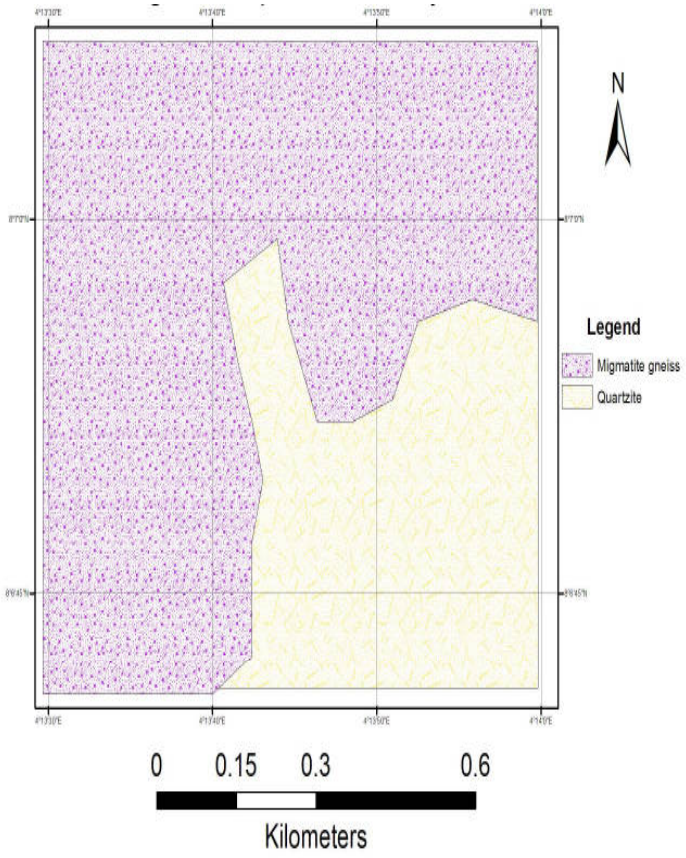

Figure 9. Geological Map of the Study Area obtained from the Interpretation of Magnetic Data

5.2.2 Quantitative Interpretation

The derived profiles (dashed lines) constructed from observed profiles (thick lines) are as shown in Figures 10a-o. The corresponding parameters obtained from the derived profiles and used in the computation of depth to magnetic source are as depicted in Tables 1 to 10. The depth to magnetic horizons as obtained from all the profiles is as summarized in Table 11. The 3- dimensional view of the depth to magnetic source of the study area is as shown in Figure 11. It indicates a depth range from about 6.1 m in the southeastern part to 10.8 m in the northeastern part of the survey area with deep magnetic basement in the west and shallow magnetic basement in the southeast and northwest.

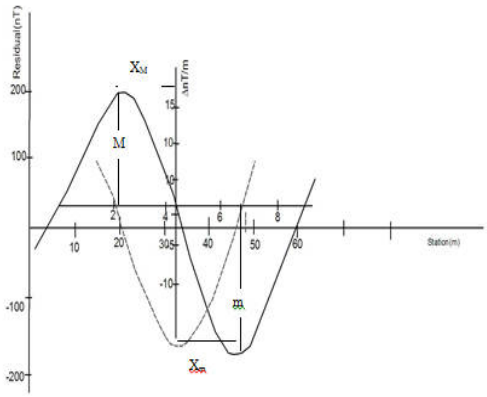

Figure 10a. Observed and Derived Profile constructed for Profile 1 (East)

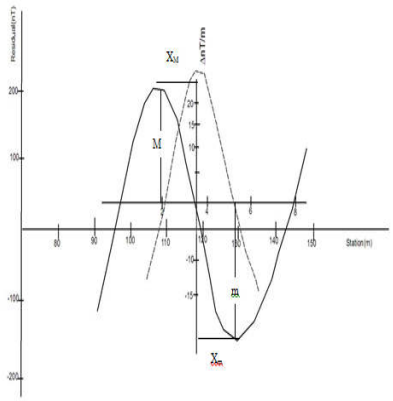

Figure 10b. Observed and Derived Profile constructed for Profile 1 (West)

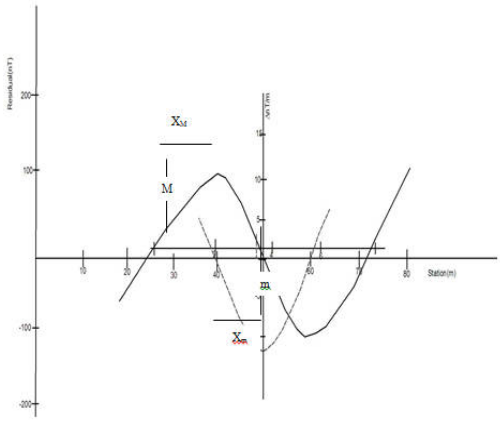

Figure 10c. Observed and Derived Profile constructed for Profile 2 (West)

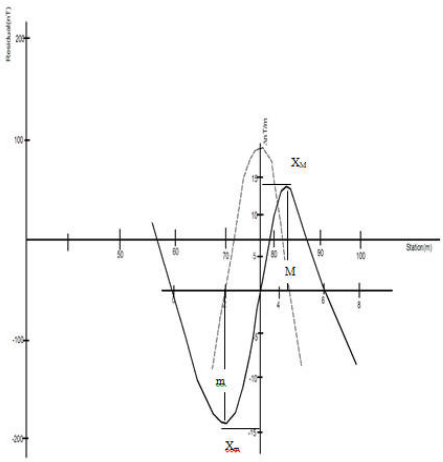

Figure 10d. Observed and Derived Profile constructed for Profile 3 (East)

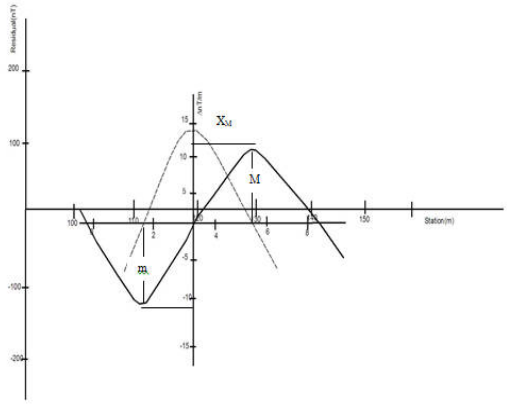

Figure 10e. Observed and Derived Profile constructed for Profile 4 (West)

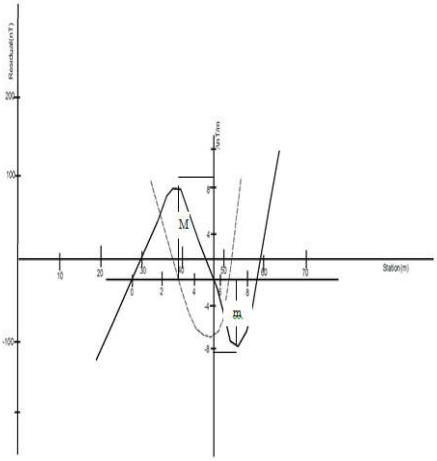

Figure 10f. Observed and Derived Profile constructed for Profile 5(East)

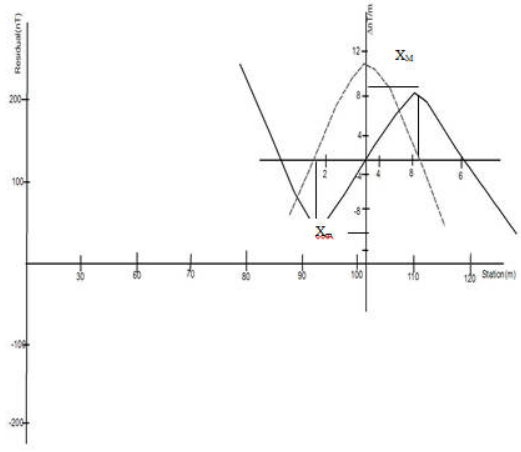

Figure 10g. Observed and Derived Profile constructed for Profile 6 (East)

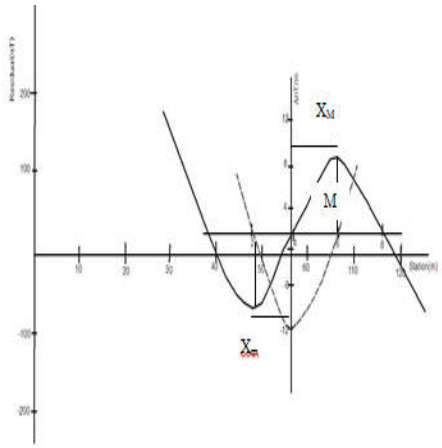

Figure 10h. Observed and Derived Profile constructed for Profile 6 (West)

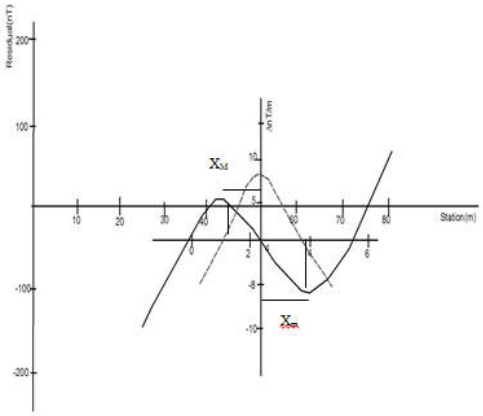

Figure 10i. Observed and Derived Profile constructed for Profile 7 (East)

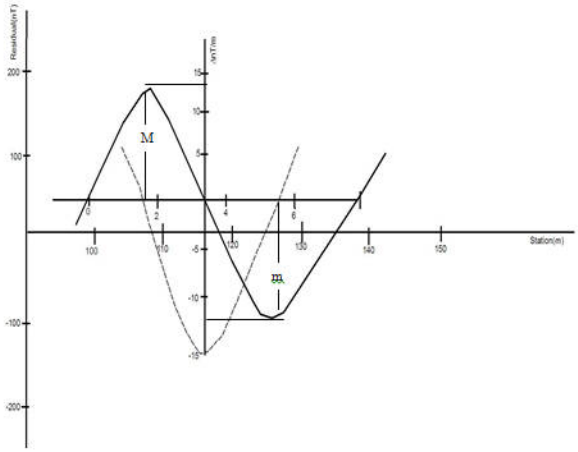

Figure 10j. Observed and Derived Profile constructed for Profile 8 (East)

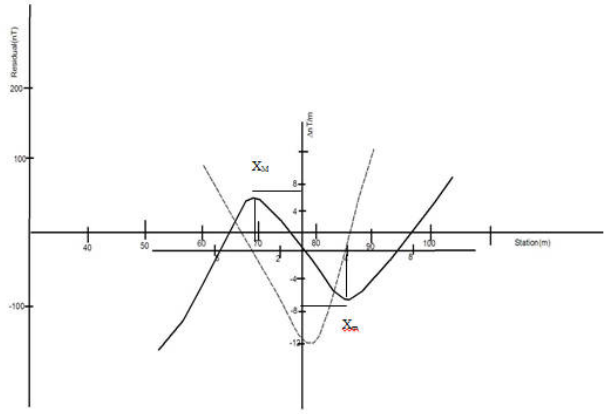

Figure 10k. Observed and Derived Profile constructed for Profile 8 (West)

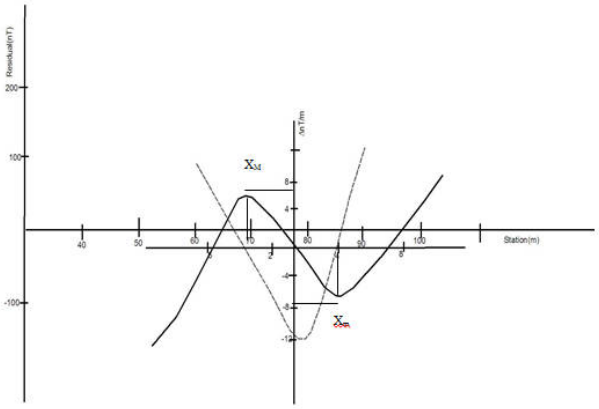

Figure 10l. Observed and Derived Profile constructed for Profile 9 (East)

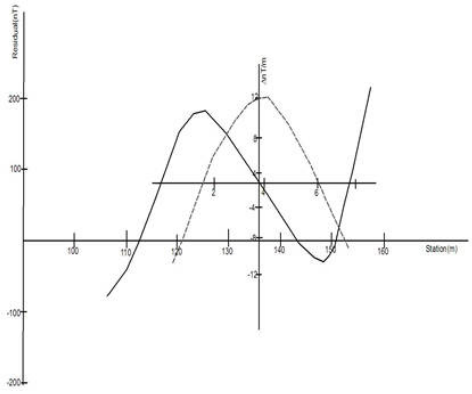

Figure 10m. Observed and Derived Profile constructed for Profile 9 (West)

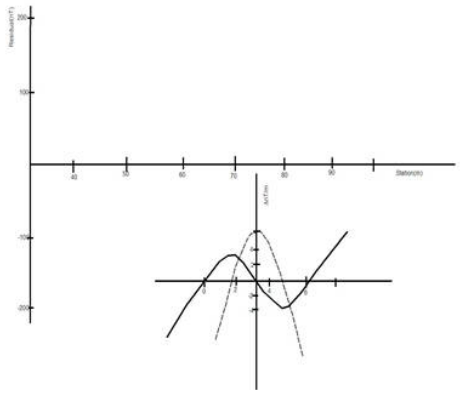

Figure 10n. Observed and Derived Profile constructed for Profile 10 (East)

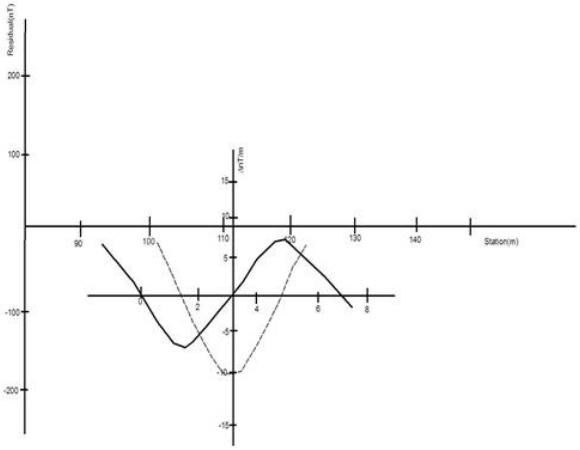

Figure 10o. Observed and Derived Profile constructed for Profile 10 (West)

Table 1.Parameters obtained from the derived profile (Profile 1)

Constructed Horizontal Scale	X_m = 5m, calculated depth = 9.3m			X_m = 5m, calculated depth = 8.3 m		
	Eastern Part			Western Part		
	Intersecting Magnetic Value (nT)	**Differential Magnetic Value (nT)**	**Vertical Scale $(X - X_o)/X_m$ (nT/m)**	**Intersecting Magnetic Value (nT)**	**Differential Magnetic Value (nT)**	**Vertical Scale $(X - X_o)/X_m$ (nT/m)**
0	226.5	-73.5	-14.7	30	-120	-24
1	300	-70	-14	150	-40	-8
2	370	-5	-1	190	80	16
3	375	80	16	110	150	30
4	295	115	23	-40	90	18
5	180	110	22	-130	-10	-2
6	70	-8	-1.6	-120	-70	-14
7	78	-82	16.4	-50	-90	-18
8	160	-105	-21	40		
9	265					

Table 2.Parameters obtained from the derived profile (Profile 2)

Constructed Horizontal Scale	X_m = 5m, calculated depth = 8.3m		
	Western Part		
	Intersecting Magnetic Value (nT)	**Differential Magnetic Value (nT)**	**Vertical Scale $(X - X_o)/X_m$ (nT/m)**
0	-142.5	-47.5	-9.5
1	-95	-40	-8
2	-55	15	3
3	-70	72.5	14.5
4	-142.5	79.5	15.9
5	-222	7	1.4
6	-229	-40	-8
7	-189	-59	-11.8
8	-130		

Table 3.Parameters obtained from the derived profile (Profile 3)

Constructed Horizontal Scale	X_m = 5m, calculated depth = 6.8 m		
	Eastern Part		
	Intersecting Magnetic Value (nT)	**Differential Magnetic Value (nT)**	**Vertical Scale $(X - X_o)/X_m$ (nT/m)**
0	-2	-22	-4.4
1	20	15	3
2	5	25	5
3	-20	5	1
4	-25	-12	-2.4
5	-13	-22	-4.4
6	9		

Table 4.Parameters obtained from the derived profile (Profile 4)

Constructed Horizontal Scale	X_m = 5m, calculated depth = 9.3 m		
	Western Part		
	Intersecting Magnetic Value (nT)	**Differential Magnetic Value (nT)**	**Vertical Scale $(X - X_o)/X_m$ (nT/m)**
0	-23.5	66.5	13.3
1	-90	38	7.6
2	-128	-58	-11.6
3	-70	-60	-12
4	-10	-50	-10
5	40	-41	-8.2
6	81	39	7.8
7	42	42	8.4
8	0	50	10
9	-5		

Table 5.Parameters obtained from the derived profile (Profile 5)

Constructed Horizontal Scale	X_m = 5m, calculated depth = 7.0 m		
	Eastern Part		
	Intersecting Magnetic Value (nT)	**Differential Magnetic Value (nT)**	**Vertical Scale $(X - X_o)/X_m$ (nT/m)**
0	-7.5	-37.5	-7.5
1	30	-40	-8
2	70	-10	-2
3	80	30	6
4	50	70	14
5	-20	70	14
6	-90	10	5
7	-100	-40	-8
8	-60	-52.5	-10.5
9	-7.5		

Table 6.Parameters obtained from the derived profile (Profile 6)

Constructed Horizontal Scale	X_m = 5m, calculated depth = 8.8 m			X_m = 5m, calculated depth = 8.8 m		
	Eastern Part			Western Part		
	Intersecting Magnetic Value (nT)	**Differential Magnetic Value (nT)**	**Vertical Scale $(X - X_o)/X_m$ (nT/m)**	**Intersecting Magnetic Value (nT)**	**Differential Magnetic Value (nT)**	**Vertical Scale $(X - X_o)/X_m$ (nT/m)**
0	126	76	15.2	27	67	13.4
1	50	-20	-4	-40	20	4
2	70	-40	-8	-60	-40	-8
3	110	-60	-12	-20	-52	-10.4
4	170	-37	-7.4	32	-63	-12.6
5	207	57	11.4	95	-23	-4.6
6	150	40	8	118	46	9.2
7	110			72	45	9.0
8				27		

Table 7.Parameters obtained from the derived profile (Profile 7)

Constructed Horizontal Scale	X_m = 5m, calculated depth = 9.3 m		
	Eastern Part		
	Intersecting Magnetic Value (nT)	**Differential Magnetic Value (nT)**	**Vertical Scale $(X - X_o)/X_m$ (nT/m)**
0	-16	-101	-20.2
1	85	-29	-5.8
2	114	56	11.2
3	58	58	11.6
4	0	53	10.6
5	-53	35	7
6	-88	-38	-7.6
7	-50	-105	-21
8	55		

Table 8.Parameters obtained from the derived profile (Profile 8)

Constructed Horizontal Scale	X_m = 5m, calculated depth = 7.8 m			X_m = 5m, calculated depth = 8.8 m		
	Eastern Part			Western Part		
	Intersecting Magnetic Value (nT)	**Differential Magnetic Value (nT)**	**Vertical Scale $(X - X_o)/X_m$ (nT/m)**	**Intersecting Magnetic Value (nT)**	**Differential Magnetic Value (nT)**	**Vertical Scale $(X - X_o)/X_m$ (nT/m)**
0	-38	-51	-10.2	38.5	-81.5	-16.3
1	13	38	7.6	120	-27	-5.4
2	-25	40	8	47	77	15.4
3	-65	24	4.8	70	80	16
4	-89	-29	-5.8	-10	69	13.8
5	-60	-75	-15	-79	-19	-3.8
6	15			-60	-70	-14
7				10	-55	-11
8				65		

Table 9.Parameters obtained from the derived profile (Profile 9)

Constructed Horizontal Scale	X_m = 5m, calculated depth = 10.8 m			X_m = 5m, calculated depth = 9.7 m		
	Eastern Part			Western Part		
	Intersecting Magnetic Value (nT)	**Differential Magnetic Value (nT)**	**Vertical Scale $(X - X_o)/X_m$ (nT/m)**	**Intersecting Magnetic Value (nT)**	**Differential Magnetic Value (nT)**	**Vertical Scale $(X - X_o)/X_m$ (nT/m)**
0	-31.5	-61.5	-12.3	69	-93	-18.6
1	30	20	4	162	-7	-1.4
2	10	60	12	169	54	10.8
3	-50	48	24	115	55	11
4	-98	-36	-7.2	60	60	12
5	-63	-47	-9.4	0	38	7.6
6	-15			-38	-68	-13.6
7				30		

Table 10.Parameters obtained from the derived profile (Profile 10)

Constructed Horizontal Scale	X_m = 5m, calculated depth = 6.1 m			X_m = 5m, calculated depth = 8.3 m		
	Eastern Part			Western Part		
	Intersecting Magnetic Value (nT)	**Differential Magnetic Value (nT)**	**Vertical Scale $(X - X_o)/X_m$ (nT/m)**	**Intersecting Magnetic Value (nT)**	**Differential Magnetic Value (nT)**	**Vertical Scale $(X - X_o)/X_m$ (nT/m)**
0	-153	-20	-4	-94.5	60.5	12.1
1	-130	-10	-2	-160	-5	-1
2	-120	30	6	-155	-51	-10.2
3	-150	22	4.4	-104	-54	-10.8
4	-172	10	2	-50	-22	-4.4
5	-182	-29	-5.8	-28	34	6.8
6				-62	48	9.6
7				-110		

Table 11. Summary of depth to magnetic horizon of all the profiles

Profile	**Depth to magnetic horizon (m)**
One (eastern part)	9.3
One (western part)	8.3
Two (western part)	8.3
Three (eastern part)	6.8
Four (western part)	9.3
Five (eastern part)	7.0
Six (eastern part)	8.8
Six (western part)	8.8
Seven (eastern part)	9.3
Eight (eastern part)	7.8
Eight (western part)	8.8
Nine (eastern part)	10.8

Nine (western part)	9.7
Ten (eastern part)	6.1
Ten (western part)	8.34

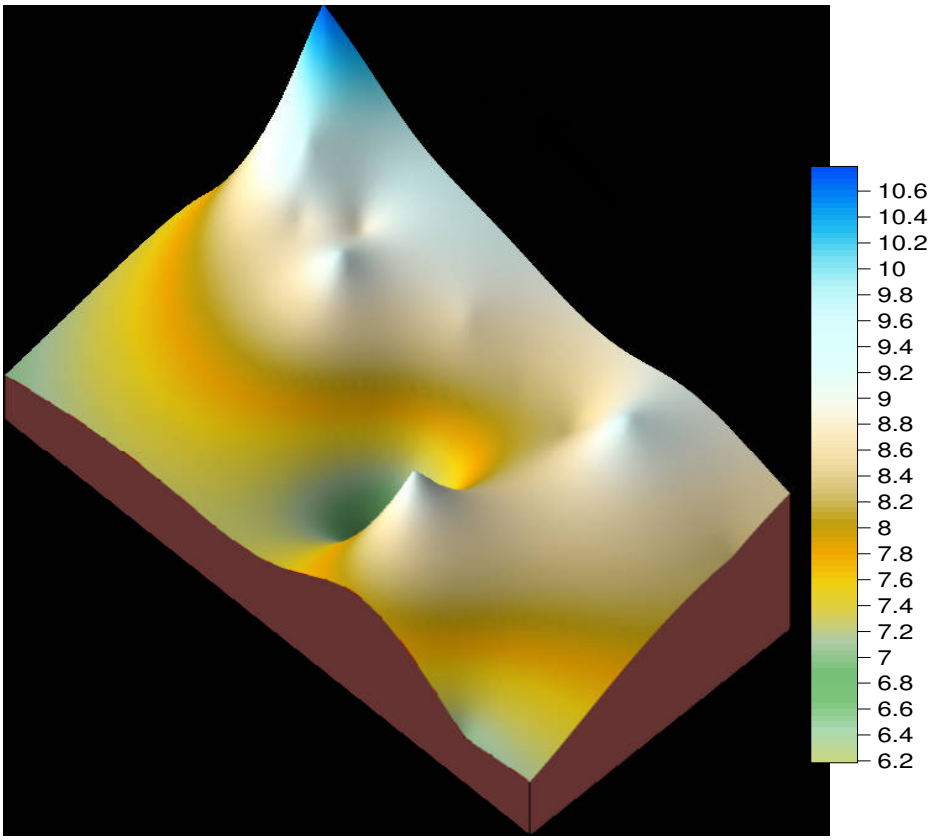

Figure 12. 3-D view of Depth to Magnetic Horizon

6. Conclusion

The magnetic method has been used to investigate subsurface geologic features of Oke Alapata area of Ogbomoso. The magnetic anomalies varied between minimum negative peak value of -400nT and maximum peak value of 520nT. The inferred geologic features include joints, fractures, and rock-rock contact between migmatite-gneiss and quartzite. The locations of migmatite-gneiss/quartzite contacts on the magnetic signatures were characterized by positive and negative anomaly peaks and agreed with the observed contact on the geological map obtained from field mapping. The depth to magnetic source ranged from 6.1m at the southeastern part to 10.8m at the northeastern part of the study area with deep magnetic basement in the west and shallow magnetic basement in the southeast and northwest.

Appendix I: Sample Calculation of depth to Basement using Pal's (1984) method

Depth to Magnetic Horizon for Profile 1 (Eastern Part)

Parameters from the graphical plot (Figure 10a) are;

M = 388nT and m = 65nT

$X_o = (m + M) / 2 = 226.5nT$

$X_m = 50m$ and $X_M = 55m$

$U=\sqrt{-(X_m \times X_M)}\ m^2$

$= \sqrt{-(-50 \times 55)}\ m^2$

$U = \sqrt{2750}\ m^2 = 52.44m$

$h= -½ (X_m + X_M) \tan \theta_F$

but $\theta_F = \pm \tan^{-1} B\sqrt{\frac{U}{X_m + X_M}}$ and B = 1.1457

yielding $\theta_F = \tan^{-1} 3.7104$

Depth $h = \pm ½ (Xm + X_M) \tan \theta_F$

h = 9.28 m

Therefore, the overburden and hence, depth to magnetic horizon = 9.3 m

Calculation of Depth to Magnetic Horizon for Profile 1 (Western part).

Parameters from the graphical plot are;

m = -136nT and M = 190nT

$X_o = (m + M) / 2 = 27nT$

$X_m = 45m$ and $X_M = 40m$

$U=\sqrt{-(X_m \times X_M)}\ m^2$

$= \sqrt{-((-45) \times 40)}\ m^2$

$U = \sqrt{1800}\ m^2 = 42.43m$

$h= -½ (X_m + X_M) \tan \theta_F$

but $\theta_F = \pm \tan^{-1} B\sqrt{\frac{U}{X_m + X_M}}$ and B = 1.1457

yielding $\theta_F = \tan^{-1} 3.3374$

Depth $h = \pm ½ (X_m + X_M) \tan \theta_F$

i.e. h = 8.3

Therefore, the overburden and hence depth to magnetic horizon = 8.3 m

Appendix II: Implementation of Porna's (1984) in JAVA

```
import java.awt.*;
import java.awt.event.*;
import javax.swing.*;
public class Desmond extends JFrame
{
        private JButton btn,cancel,btnExit,btnBack;
        private JTextField hd_m,hd_M;
        private CardLayout card;
        private JPanel panelEx,CentralPanel;
        private double u;
        private final double B_Const = 1.1457;
        private JLabel uLabel;

  public Desmond()
  {
        setTitle("Magnetic Horizon");
```



```
        setSize(700,400);
        setLocationRelativeTo(null);
        setVisible(true);
        setDefaultCloseOperation(JFrame.EXIT_ON_CLOSE);
        setResizable(false);
        card = new CardLayout();
        CentralPanel = new JPanel(card);
        JPanel first = new JPanel(new GridBagLayout());
        GridBagConstraints g = new GridBagConstraints();
        JLabel title = new JLabel("Pal's Method for Depth To Magnetic Horizon");
        title.setFont(new Font("Courier new",Font.BOLD,18));
        g.gridx = 0;
        g.gridy = 0;
        first.add(title,g);
                g.gridx = 0;
        g.gridy = 1;
        first.add(mainPanel(),g);
        CentralPanel.add("FirstCard",first);
        panelEx = new JPanel();
        JLabel title2 = new JLabel("Pal's Method for Depth To Magnetic Horizon");
        title2.setFont(new Font("Courier new",Font.BOLD,18));
        panelEx.add(title2);
        CentralPanel.add("second",secondPanel());
        add(CentralPanel);
}
public JPanel mainPanel()
{
        JPanel panel = new JPanel(new GridBagLayout());
        panel.setBorder(BorderFactory.createTitledBorder("Compute"));
        panel.setPreferredSize(new Dimension(500,300));
        GridBagConstraints gbc = new GridBagConstraints();
        gbc.insets = new Insets(5,5,5,5);
        JLabel label1 = new JLabel("Horizontal Distance of (m) to DC (X_m):");
        gbc.gridx = 0;
        gbc.gridy = 0;
        panel.add(label1,gbc);
        hd_m = new JTextField(15);
        gbc.gridx = 1;
        gbc.gridy = 0;
        panel.add(hd_m,gbc);
        JLabel label2 = new JLabel("Horizontal Distance of (M) to DC (X_M):");
        gbc.gridx = 0;
```



```
gbc.gridy = 1;
panel.add(label2,gbc);
hd_M = new JTextField(15);
gbc.gridx = 1;
gbc.gridy = 1;
panel.add(hd_M,gbc);
btn = new JButton("Next");
btn.addActionListener(new ActionListener()
        {
                public void actionPerformed(ActionEvent evt)
                {
                        double double_hd_m = Double.parseDouble(hd_m.getText());
                        double double_hd_M = Double.parseDouble(hd_M.getText());
                        double positive_hd_m  = -(double_hd_m);
                        u = Math.sqrt(positive_hd_m * double_hd_M);
                        double add = double_hd_m+double_hd_M;
                        double b1 = 0;
                        double h1 = 0;
                        double  theta1 = 0;
                        if(add > 0)
                        {
                                b1 = B_Const * Math.sqrt(u/(add));
                                theta1 = Math.atan(b1);
                                h1 = (0.5)*((double_hd_m+double_hd_M)*b1);
                        }
                        else
                        {
                                b1 = B_Const * Math.sqrt(u/-(add));
                                theta1 = Math.atan(b1);
                                h1 = -(0.5)*((double_hd_m+double_hd_M)*b1);
                        }

                        String s = String.valueOf(h1);
                        uLabel.setText(s);
                        card.show(CentralPanel,"second");
                }
        });
btnExit = new JButton("Exit");
btnExit.addActionListener(new ActionListener()
{
        public void actionPerformed(ActionEvent evt)
                {
```



```
                                System.exit(0);
                        }
        });
        cancel = new JButton("Cancel");
        cancel.addActionListener(new ActionListener()
        {
                public void actionPerformed(ActionEvent evt)
                        {
                                hd_m.setText(null);
                                hd_M.setText(null);
                        }
        });
        JPanel btnPanel = new JPanel();
        btnPanel.add(btn);
        btnPanel.add(cancel);
        btnPanel.add(btnExit);
        gbc.gridx = 0;
        gbc.gridy = 2;
        gbc.gridwidth = 2;
        panel.add(btnPanel,gbc);
        return panel;
}
private JPanel secondPanel()
{
        JPanel panel = new JPanel(new GridBagLayout());
        GridBagConstraints gbc = new GridBagConstraints();
        JPanel secondInternalPanel = new JPanel(new GridBagLayout());
        secondInternalPanel.setBorder(BorderFactory.createTitledBorder("Compute The Value of h "));
        secondInternalPanel.setPreferredSize(new Dimension(500,300));
        uLabel = new JLabel();
        uLabel.setFont(new Font("courier new",Font.BOLD,20));
        gbc.gridx = 0;
        gbc.gridy = 0;
        secondInternalPanel.add(uLabel,gbc);
        btnBack = new JButton("Back");
        btnBack.addActionListener(new ActionListener()
        {
                public void actionPerformed(ActionEvent evt)
                {
                        card.show(CentralPanel,"FirstCard");
                }
        });
```



```
                gbc.gridx = 0;
        gbc.gridy = 1;
        secondInternalPanel.add(btnBack,gbc);
        JLabel labelSecondTitle = new JLabel("Pal's Method for Depth To Magnetic Horizon");
        labelSecondTitle.setFont(new Font("Courier new",Font.BOLD,18));
        gbc.gridx = 0;
        gbc.gridy = 0;
        panel.add(labelSecondTitle,gbc);
        gbc.gridx = 0;
        gbc.gridy = 1;
        panel.add(secondInternalPanel,gbc);
        return panel;
  }
  private static void laf()
  {
        try
        {
                UIManager.setLookAndFeel(UIManager.getSystemLookAndFeelClassName());
                }
                catch (Exception ex)
                {

                }
  }
  public static void main (String[] args)
        {
                SwingUtilities.invokeLater(new Runnable()
                {
                        public  void run()
                        {
                                laf();
                                new Desmond();
                        }
                });
        }
}
```

References

Afolabi, O. A., Kolawole, L. L., Abimbola A. F., Olatunji, A. S. & Ajibade, O. M. (2013), "Preliminary Study of the Geology and Structural Trends of Lower Proterozoic Basement rocks in Ogbomoso, SW Nigeria'', *Journal of Environment and Earth Science* **3**(8), 82-95.

Frischknecht, F.C. & Raab, P.V. (1984), "Location of abandoned wells by magnetic surveys'', *Proceedings, 1st National Conference on Abandoned wells – Problems and solutions*. Environmental and Groundwater Institute,

186-215

Frischknecht, F.C. (1990), "Application of geophysical methods to the study of pollution associated with abandoned and injection wells", *Proceedings of a U.S. Geological Survey Workshop on Environmental Geochemistry*. U.S. Geological survey Circular 1033, 73-77

Hinze, W. J., 1990. The Role of Gravity and Magnetic Methods in Engineering and Environmental Studies. In: Ward, S. (ed.) Geotechnical and Environmental Geophysics, Society of Exploration Geophysicists, Tulsa, OK, pg 75-126.

Jones, H.A. & Hockey, R.D. (1964), "The geology of the southwestern Nigeria", *Geol. Surv. Nig. Bull* **31**, 101.

Kearey, P., Brooks M. & Hill, I. (2002), "An Introduction to geophysical exploration", (3rd edition) Black well scientific publication, Oxford

Olaseinde, P. I. (1990), "A spectral evaluation of the aeromagnetic anomaly map over part of the Nigerian Basement complex", *Ph.D thesis*, University of Ilorin, Ilorin Nigeria.

Pal, P. C. (1984), "A gradient analysis based simplified inversion strategy for the magnetic anomaly of an inclined and infinite thick dyke", *Geophysics* **50**(7), Society of Exploration Geophysicists, 1179-1182.

Prieto, C. & Morton, G.. (2003), "New insights from a 3D earth model, deepwater Gulf of Mexico", *The Leading Edge* **22**, Society of Exploration Geophysicists, 356-360

Rahaman, M.A. (1989), "A review of the geology of southwestern Nigeria", In: Geology of Nigeria (C.A Kogbe ed.) Elizabeth Press. 39-55

Schmidt, A. (2001), "Visualisation of multi-source archeological geophysics data", In: Cucarzi, M. and Conti, P. (eds) Filtering, Optimization and Modelling of Geophysical Data in Archeological Prospecting, Rome. Fondazione Ing. Carlo M. Lerici, pg. 149-160

Schmidt, A., Yarnold, R., Hill, M. & Ashmore, M. (2005), "Magnetic susceptibility as proxy for heavy metals pollution: A site study", *Geochemical Exploration* **85**, Elsevier, 109-117

Soengkono, S. & Hochstein, M.P. (1995), "Application of Magnetic method to assess the extent of high temperature geothermal reservoirs", *Proceedings on 20th workshop on geothermal reservoir engineering*, 71-78

Sternberg, R.S. (2001), "Magnetic properties and archeomagnetism", In: Brothwell, D.R.and Pollard, A.M. (eds.) Handbook of Archeological Sciences, Chichester John Willey and Sons Limited.

Sunmonu, L.A., Adabanija, M.A. & Olowofela, J.A. (2001), "2-dimensional spectral analysis of aeromagnetic data over southeastern part of Bida basin Nigeria", *Nigerian Journal of Physics.***12**, 39-44

Sunmonu, L.A., Adabanija, M.A., Kumar, D.P. & Olowofela, J.A. (2004), "Estimation of Basement depths beneath the Koton-karifi Area of Bida Basin (Nigeria) from Aeromagnetic data", *Journal of Geophysics,* Association of Exploration Geophysicists, 19-26

Sutherland, T. & Schmidt, A. (2003), "Towton, 1461: An integrated approach to Battlefield Archeology", *Landscapes* **4**, 15-25

Telford, W. M., Geldart, L.P. & Sheriff, R.E. (1990), "Applied Geophysics", (2nd ed.). New York: Cambridge University Press

Xia, J. & Williams, S.L. (2003), "High-resolution magnetic survey in locating abandoned brine wells in Hutchinson, Kansas", Symposium on the Application of Geophysics to Engineering and Environmental problems (SAGEEP) 2003 Annual Meeting of EEGS, April 6-10, 2003 San Antoniuo, Texas, 12pp.

Xia, J. & Williams, S.L. (2004), "High-resolution magnetic survey in locating abandoned brine wells in Hutchinson, Kansas", In: Johnson, K.S. and Neal, J.T. (eds) Evaporate Karst and Engineering and Environmental Problems in the United States. Oklahoma Geological Survey Circular 109, pg. 169-175

Xia, J., Chen, C., Xia, S. & Laflen, D. (2003), "Applications of high resolution magnetic method and gradient method in locating abandoned brine wells in Hutchinson, Kansas", Kansas Geological Survey Open-file report 2003-48

Xia, J., Chen, C., Xia, S., Laflen, D. & Williams, S.L. (2004), "Using high- resolution magnetic method and gradient method to locate abandoned brine wells in Hutchinson, Kansas", Symposium on the application of Geophysics to Engineering and Environmental Problems (SAGEEP) 2004 Annual Meeting of EEGS, February 22-26, Colorado Springs, Colorado pg. 1350-1367